

Online Appendix to  
“Can Structural Small Open-Economy Models  
Account for the Influence of Foreign Disturbances?”

Alejandro Justiniano      Bruce Preston

December 4, 2009

This appendix provides further details on two aspects of the paper.

Section 1 analyzes the robustness of our results when computing simulated — as opposed to population — moments and shows that our conclusions remain unaltered. A technical discussion follows, highlighting the need to be cautious in comparing simulated cross-country correlations and variance decompositions.

In section 2, we provide further details on the prior and posterior properties of the model which form the basis of section 8 of the paper.

## **1 Simulated versus Population Moments**

Sections 2 and 5 of the paper contrast the empirical and baseline model-implied population cross-correlations between Canadian and U.S. series, accounting for the uncertainty surrounding model parameters. Here we revisit these comparisons focusing instead on simulated model-implied moments, which account for both parameter and small-sample uncertainty. These statistics are computed with the draws from the posterior distribution of the DSGE parameters, where for each draw we simulate a single artificial sample of length equal to the data (after discarding 100 initial observations to remove any dependence from initial conditions).

Figure 1A — with A here and subsequently signifying a table or figure appearing in this appendix — presents the small-sample analogue to figure 1 of the paper, where the latter is based on population moments. We report median (dotted) and [5,95] percent posterior probability bands (dashed).<sup>1</sup> Not surprisingly, the median of simulated model-implied cross-correlations are still virtually zero at all horizons. More interestingly, the posterior probability bands are far wider here relative to those in figure 1. We shall return to this issue in the next subsection. Nonetheless, for many Canadian series, the data cross-correlations lie outside the posterior probability bands of the corresponding model statistics. This is evident in the cross-correlations between Canadian output, nominal interest rates and wages and their U.S. counterparts. Similarly the contemporaneous correlation between inflation in the two countries is poorly fit. Many of the remaining cross-correlations are not well matched. Even for moments where the posterior bands encompass the data, it is rarely true (except for hours) that the data correlation is close to zero.

Table 1A presents the simulated variance decomposition for the stationary (or long-horizon) variance, for the same draws and artificial samples as above. Each decomposition is obtained by feeding one shock at a time (for each parameter draw and associated artificial sample), computing the resulting variances and summing them across domestic and foreign shocks. The two columns represent different ways of computing the total variance (in the denominator) due to the small-sample correlation present in each simulation amongst components that should be orthogonal in population, an issue discussed at length in the next subsection. For current purposes it suffices to note that this is the small-sample analogue of the last column in table 3 of the paper, which is based on population moments.

The median estimates for the share of variance explained by foreign shocks are identical (to 2 decimal places) across simulated and population moments (regard-

---

<sup>1</sup>By posterior we refer to sample moments computed using the posterior distribution of parameter draws. The notion of small-sample uncertainty arising from repeated replications of a data generating process, at a given point in the parameter space (such as the mode) is instead a frequentist object.

less of how the denominator is computed for the former). The posterior probability bands are only slightly larger with simulation-based variance decompositions. Even when accounting for small-sample uncertainty the model is unable to account for the influence of foreign shocks. These exercises constitute important robustness checks on our results.

Nonetheless, it is intriguing that introducing small-sample uncertainty induces larger changes for the cross-correlations than for the variance decompositions (relative to the population analogues). While medians are essentially identical in population or simulation for both moments, posterior probability bands for the cross-correlations widen considerably when using simulated moments. This is not the case for the variance decompositions.

At first glance, therefore, the simulated cross-correlations and variance decompositions would seem to provide a less cohesive view than when relying solely on population moments. The remainder of this section clarifies the source of this discrepancy. Before providing details it is important to note that this is a technical issue that concerns only the width of the posterior bands for the simulated cross-correlations. It arises from the presence of a “spurious” component in small samples which is not present in population (or very large samples). While our conclusions remain unaltered, the discussion highlights that making inferences about some aspects of the model can require care in the presence of small-sample uncertainty. For readers less interested in technical issues, we preview that correcting for this spurious component in figure 6A delivers posterior bands for the cross-correlations more in line with those reported in figure 1, as well as with the posterior bands for the simulated variance decompositions. The discussion below also provides greater detail on the comparison between population and simulated moments and on the construction of the later.

## 1.1 A simple model

Consider the following simple static model which suffices to illustrate conceptual issues without the complication of dynamics.<sup>2</sup> Let  $y_{1,t}$  and  $y_{2,t}$  denote U.S. and Canadian output and  $\varepsilon_{1,t}$  and  $\varepsilon_{2,t}$  denote the mean-zero column vector of U.S. and Canadian disturbances at time  $t$ , assumed *orthogonal* to each other. The small open-economy assumption, without dynamics, permits output in each country to be modeled as

$$\begin{aligned} y_{1,t} &= a' \varepsilon_{1,t} \\ y_{2,t} &= b' \varepsilon_{1,t} + d' \varepsilon_{2,t} \end{aligned}$$

where the column vectors  $a$ ,  $b$  and  $d$  are of appropriate size, while  $\Sigma_{11} = E(\varepsilon_{1,t} \varepsilon_{1,t}')$ ,  $\Sigma_{22} = E(\varepsilon_{2,t} \varepsilon_{2,t}')$  and  $\Sigma_{12} = E(\varepsilon_{1,t} \varepsilon_{2,t}')$ .

Two types of model-based moments can be obtained. First, *population* moments, computed using the formulas corresponding to the state-space representation of the model's solution. Second, *simulated* (or sample) moments, obtained by generating artificial samples across multiple replications and reporting measures of location and dispersion from the resulting distribution of sample statistics. More formally, let  $\{\varepsilon_{1,t}^j, \varepsilon_{2,t}^j\}_{t=1}^T$  denote the artificial set of disturbances generated in replication  $j$  (out of  $J$  total) with the covariance matrices given above. These disturbances generate sequences  $\{y_{1,t}^j, y_{2,t}^j\}_{t=1}^T$  from which the corresponding sample statistics are computed. Simulated moments will be denoted by the accent “ $\hat{\phantom{x}}$ ” to distinguish them from their population counterparts.

While conditional on a given vector of structural parameters (which determines  $a$ ,  $b$  and  $d$ ) the population moments are fixed, simulated moments will vary across replications. Therefore, the posterior distribution of simulated moments (obtained using the posterior parameter draws) also accounts for small-sample uncertainty.

It is useful to employ the following decomposition. Let  $\{y_{1,\varepsilon_1,t}^j, y_{2,\varepsilon_1,t}^j\}_{t=1}^T$  denote the series obtained when there are only foreign shocks,  $\varepsilon_{1,t}$ . Similarly let

---

<sup>2</sup>We are very grateful to one of the referees for suggesting this framework to analyze the discrepancy between the uncertainty surrounding variance decompositions and the cross-correlations.

$\{0, y_{2,\varepsilon_2,t}^j\}_{t=1}^T$  denote the series when there are only domestic disturbances,  $\varepsilon_{2,t}$ . Clearly  $y_{1,\varepsilon_2,t}^j = 0$  by the small open-economy assumption. This permits the representation

$$\begin{aligned} y_{1,t}^j &= y_{1,\varepsilon_1,t}^j \\ y_{2,t}^j &= y_{2,\varepsilon_1,t}^j + y_{2,\varepsilon_2,t}^j \end{aligned}$$

Population variances are

$$\begin{aligned} V(y_1) &= a'\Sigma_{11}a \\ V(y_2) &= V(y_{2,\varepsilon_1}) + V(y_{2,\varepsilon_2}) + 2Cov(y_{2,\varepsilon_1}, y_{2,\varepsilon_2}) \\ &= b'\Sigma_{11}b + d'\Sigma_{22}d + 2b'\Sigma_{12}d \\ &= b'\Sigma_{11}b + d'\Sigma_{22}d \end{aligned}$$

as the population matrix  $\Sigma_{12}$  has all entries equal to zero.

Let  $\widehat{\Sigma}_{11}^j$ ,  $\widehat{\Sigma}_{12}^j$  and  $\widehat{\Sigma}_{22}^j$  denote the sample covariances across the generated disturbances in replication  $j$ . The simulated variances are then given by

$$\begin{aligned} \widehat{V}^j(y_1) &= a'\widehat{\Sigma}_{11}^j a \\ \widehat{V}^j(y_2) &= b'\widehat{\Sigma}_{11}^j b + d'\widehat{\Sigma}_{22}^j d + 2d'\widehat{\Sigma}_{12}^j b \end{aligned}$$

where the last term in  $\widehat{V}^j(y_2)$  is equal to  $2\widehat{Cov}(y_{2,\varepsilon_1}, y_{2,\varepsilon_2})$ . This sample moment need not be zero for each replication due to the small sample cross-correlation amongst these components. Nonetheless, it will converge to zero in probability as  $T$  goes to infinity. While this small-sample correlation may be easy to control for in a static set-up (by orthogonalizing the disturbances), it cannot be avoided in a dynamic model as ours.

### 1.1.1 Variance Decompositions

The population variance shares of  $y_{2,t}$  attributed to foreign and domestic shocks are

$$\begin{aligned} sh_{y_{2,\varepsilon_1}} &= V(y_{2,\varepsilon_1})/V(y_2) = b'\Sigma_{11}b/V(y_2) \\ sh_{y_{2,\varepsilon_2}} &= V(y_{2,\varepsilon_2})/V(y_2) = d'\Sigma_{22}d/V(y_2). \end{aligned}$$

The simulated counterparts are given by

$$\begin{aligned}\widehat{sh}_{y_2,\varepsilon_1} &= b'\widehat{\Sigma}_{11}b/\widehat{V}(y_2) \\ \widehat{sh}_{y_2,\varepsilon_2} &= d'\widehat{\Sigma}_{22}d/\widehat{V}(y_2),\end{aligned}$$

dropping the replication specific subscript  $j$  for convenience.

While the population shares will always add up to one, the simulated shares will not, due to the presence of  $2d'\widehat{\Sigma}_{12}b$  in the denominator. The simulated shares will add up to  $1 - (2\widehat{cov}(y_{2,\varepsilon_1}, y_{2,\varepsilon_2})/\widehat{V}(y_2))$ . On average across replications, the second term will be zero, but not necessarily in each artificial sample. One way of circumventing this problem is to instead use  $\widehat{V}(y_{2,\varepsilon_1}) + \widehat{V}(y_{2,\varepsilon_2})$  in the denominator. Below we gauge whether this affects our results.

Regardless of this issue, the location (e.g. mean or median) of the simulated distribution of the variance decompositions should be close to the corresponding population moments. Furthermore, as  $T$  increases this distribution should concentrate more tightly around the population moment.

Subsequent computations of population and sample moments use the mode of our baseline model. While the above formulas are derived for a static model, analogous, but more cumbersome formulas, could be derived for our dynamic model. Regardless, the same issues arise between population and sample moments.

Figure 2A reports the non-parametric simulated variance decompositions of Canadian output in our model, at the mode of the parameter values, using the same sample size as in our data set and  $J = 5000$  replications. Panel A shows the histogram for the variance share attributed to all U.S. shocks, when  $\widehat{V}(y_{2,\varepsilon_1}) + \widehat{V}(y_{2,\varepsilon_2})$  is in the denominator. The solid vertical line corresponds to the population variance share. This line coincides with the median of the distribution of simulated variance decompositions. Panel B reports the variance decomposition using  $\widehat{V}(y_2)$  in the denominator which results in a very similar histogram. Regardless of which measure is used in the denominator to construct the shares, foreign shocks explain a very small fraction of Canadian output fluctuations. Furthermore, these distributions, which account for small-sample uncertainty, are fairly

tight.<sup>3</sup> We will later compare them with those for the simulated cross-correlations.

Panel C reports the empirical distribution and theoretical share (vertical line) of Canadian output explained by all domestic shocks, when  $\hat{V}(y_{2,\varepsilon_1}) + \hat{V}(y_{2,\varepsilon_2})$  is used as the denominator (shares in panels A and C sum up to 1 for each replication). Panel D shows the ratio  $(\hat{V}(y_{2,\varepsilon_1}) + \hat{V}(y_{2,\varepsilon_2})) / \hat{V}(y_2)$ . This helps gauge the problems induced by small-sample correlation amongst components which are orthogonal in population. These distortions are not severe.

### 1.1.2 Cross-Correlations

The population cross-correlation between U.S. and Canadian output is given by

$$\rho = \frac{a'\Sigma_{11}b}{(V(y_2)V(y_1))^{\frac{1}{2}}}$$

while the simulated counterpart is

$$\hat{\rho} = \frac{\widehat{cov}(y_{1,\varepsilon_1}, y_{2,\varepsilon_1}) + \widehat{cov}(y_{1,\varepsilon_1}, y_{2,\varepsilon_2})}{(\hat{V}(y_2)\hat{V}(y_1))^{\frac{1}{2}}} \quad (1)$$

$$= \frac{a'\hat{\Sigma}_{11}b + a'\hat{\Sigma}_{12}d}{(\hat{V}(y_2)\hat{V}(y_1))^{\frac{1}{2}}} \quad (2)$$

Relative to the population moment, both the numerator and denominator of  $\hat{\rho}$  are affected by the small-sample cross-correlation of the artificial observations. In population, the second term in the numerator  $\widehat{cov}(y_{1,\varepsilon_1}, y_{2,\varepsilon_2})$  will be zero, since these components are orthogonal. The implications of this “spurious” covariance term are analyzed in the next subsection.

Panel A in figure 3A reports the distribution of simulated cross-correlations between U.S. and Canadian output in our model (once again at the mode of the parameters, for 5000 replications). This distribution is similar to that reported in

---

<sup>3</sup>At the mode of the posterior density of model parameters, strictly speaking there is no *posterior* distribution of simulated statistics, since this is a frequentist concept (see footnote 1). Except insofar as that the label of *posterior* is used to signal that the model parameters underlying the replications corresponds to a measure of location from a posterior, as opposed to a prior, density.

figure 1A, since parameter uncertainty does not substantially widen these uncertainty bands. The vertical line corresponds to the population correlation (equal to 0.07) which is very close to the median of the simulated distribution.

Panel B provides a scatter plot of the absolute value of  $\hat{\rho}$  in the horizontal axis, with the square root of  $\widehat{sh}_{y_2, \varepsilon_1}$  (with  $\widehat{V}(y_2)$ , in the denominator), together with the 45 degree line, for each for the 5000 simulated samples. In population, at least in this static set-up, it must be that  $|\rho| \leq \sqrt{sh_{y_2, \varepsilon_1}}$ . But this is clearly not the case for the simulated moments, and the discrepancy would seem to be too large to be explained simply by the presence of dynamics on our model. Put another way, the *small sample* uncertainty bands for the *simulated* cross-correlations would seem to be too wide, even relative to those of the *simulated* variance shares. Furthermore, the discrepancy would seem unlikely to correspond solely to the presence of dynamics in our model (which of course delivers more cumbersome formulas than the ones presented with this static set-up).

### 1.1.3 Spurious covariances and cross-correlations

From equation (1) it is possible to decompose the sample cross-correlation of U.S. and Canadian output into 2 components

$$\hat{\rho} = \frac{\widehat{cov}(y_{1, \varepsilon_1}, y_{2, \varepsilon_1})}{(\widehat{V}(y_2)\widehat{V}(y_1))^{\frac{1}{2}}} + \frac{\widehat{cov}(y_{1, \varepsilon_1}, y_{2, \varepsilon_2})}{(\widehat{V}(y_2)\widehat{V}(y_1))^{\frac{1}{2}}}$$

If the second term were zero, as in population, then  $\hat{\rho}$  would equal

$$a'\widehat{\Sigma}_{11}b/(\widehat{V}(y_2)\widehat{V}(y_1))^{\frac{1}{2}}$$

This “true component” of the output cross-correlation would be affected in small samples only to the extent that  $\widehat{V}(y_2)$  is different from  $\widehat{V}(y_{2, \varepsilon_1}) + \widehat{V}(y_{2, \varepsilon_2})$ . The analysis of the simulated variance decompositions suggests this distortion in simulated statistics is likely to be small.

Panel A in figure 4A replicates the distribution of simulated  $\hat{\rho}$  reported in the previous figure, while panel B provides a histogram of the “true component”  $\widehat{cov}(y_{1, \varepsilon_1}, y_{2, \varepsilon_1})/(\widehat{V}(y_2)\widehat{V}(y_1))^{\frac{1}{2}}$  for the same replications. The distribution of the

true component of the cross-correlation is substantially more concentrated than that of  $\widehat{\rho}$ . Panel C shows it is now the case that

$$|\widehat{cov}(y_{1,\varepsilon_1}, y_{2,\varepsilon_1}) / (\widehat{V}(y_2)\widehat{V}(y_1))^{\frac{1}{2}}| \leq \sqrt{\widehat{sh}_{y_2, \varepsilon_1}},$$

when  $\widehat{V}(y_2)$  is used in the denominator of both sample statistics. Note also that the median in panel B coincides with the population cross-correlation (vertical line).

Therefore the discrepancy between the width of the uncertainty bands for simulated variance shares and output cross-correlations arises from the “spurious” small sample simulation covariance  $\widehat{cov}(y_{1,\varepsilon_1}, y_{2,\varepsilon_2})$ , which is zero in population or large samples. We refer to it in this way since it can be more formally understood using the tools developed to analyze spurious regressions with persistent but stationary series in Granger, Namwon, and Yongil (2001). Using the set-up of that paper, and switching to a dynamic case as in our model, suppose

$$y_{1,\varepsilon_1,t} = \theta_1 y_{1,\varepsilon_1,t-1} + \varepsilon_{1,t}$$

and

$$y_{2,\varepsilon_2,t} = \theta_2 y_{2,\varepsilon_2,t-1} + \varepsilon_{2,t},$$

where  $|\theta_1| < 1$ ,  $|\theta_2| < 1$ , while  $\varepsilon_{1,t}$  and  $\varepsilon_{2,t}$  are i.i.d. zero mean with associated variances  $\sigma_{\varepsilon_1}^2$  and  $\sigma_{\varepsilon_2}^2$ . As in our model,  $y_{1,\varepsilon_1}$  and  $y_{2,\varepsilon_2}$  are orthogonal in population.

From their theorem 1 (page 901) the simulated covariance between these two orthogonal components has asymptotic properties

$$\sqrt{T}\widehat{cov}(y_{1,\varepsilon_1}, y_{2,\varepsilon_2}) \rightarrow^d N\left(0, \frac{1 - \theta_1^2\theta_2^2}{(1 - \theta_1\theta_2)^2} \frac{\sigma_{\varepsilon_2}^2}{1 - \theta_2^2} \frac{\sigma_{\varepsilon_1}^2}{1 - \theta_1^2}\right).$$

The covariance statistic will be a consistent estimator but its small-sample distribution will have a standard deviation increasing in the degree of persistence of the series involved. For detrended output, which is quite persistent, and our sample size, the standard deviation for  $\widehat{cov}(y_{1,\varepsilon_1}, y_{2,\varepsilon_2})$  is above 1.5 (with mean zero). This helps explain why the distorted width of the posterior probability bands (using the posterior parameter draws) relative to the true component is more severe in

the case of Canadian output than, say, Canadian inflation, which is less persistent (compare figures 1 and 1A).

Panel D shows the histogram for  $\widehat{cov}(y_{1,\varepsilon_1}, y_{2,\varepsilon_2})/(\widehat{V}(y_2)\widehat{V}(y_1))^{\frac{1}{2}}$ . For each replication, the simulated moments in panels B and D add up to those of panel A. It is clear that the dispersion of the simulated cross-correlation  $\widehat{\rho}$  comes from the spurious covariance in the last panel.

An alternative simulated estimate of the output cross-correlation which circumvents the spurious covariance is

$$\frac{\widehat{cov}(y_{1,\varepsilon_1}, y_{2,\varepsilon_1})}{(\widehat{V}(y_{2,\varepsilon_1}) + \widehat{V}(y_{2,\varepsilon_2}))\widehat{V}(y_1)^{\frac{1}{2}}}$$

As in the case of the variance decompositions, this change in denominator results in a histogram that is virtually indistinguishable from that in panel B. It is also true that the absolute value of this statistic (not shown) is less than the square root of the variance share computed using the same denominator (recall this resolves the sample correlation issues in simulated variance decompositions).

#### 1.1.4 Further Consistency Checks

As a final piece of evidence, figure 5A reports the histogram of simulated variance shares, as well as the raw and “true” components of the output cross-correlations for 5000 replications using a sample of  $T = 1000$ . Population moments again correspond to vertical lines. As expected, with this larger sample size, the distribution of simulated statistics shrinks towards the population moments. However, the histogram of the simulated output cross-correlations (panel C) is still substantially wider than the histogram for its true component (panel D). This is consistent with Granger et al’s findings that the problem posed by spurious covariances will remain in very large samples if the variables involved are quite persistent.

#### 1.1.5 Revisiting simulated cross-correlations

Based on the previous analysis, and for completeness, we revisit the computation of simulated cross-correlations over the parameter draws. Figure 6A reports the

“true” component of the simulated cross-correlations using the same draws and replication settings as in figure 1A (which did not perform this adjustment). Now the width of the posterior probability bands is only somewhat larger than for the population moments and in line with the posterior bands for the simulated variance decomposition — compare table 1A.

## 2 Prior and Posterior Comparisons

Section 8 of the paper analyzes prior implied cross-correlations to shed light on possible reasons why posterior estimates from specifications without correlated shocks shut down international linkages. As discussed, we conduct this investigation in a version of the model which pre-estimates the U.S. block. Using very tight “priors” around the posterior mode of this initial step, the domestic block is then estimated.

The purpose of this two-step procedure is to obtain a “prior” (in stark violation of the principle of eliciting information *before* observing the data) which is highly informed on which foreign shocks are responsible for generating comovement and their implications. We generate random draws from this prior to obtain a distribution of prior (population) cross-correlations, impulse responses and variance decompositions, which helps us understand the transmission mechanisms embedded in the model.

Figure 7A presents selected prior cross-correlations both between U.S. and Canada, as well as several within the domestic block, that are referenced in section 8. Each panel shows the median and [5,95] bands from the *prior* distribution of population cross-correlations (dotted and dashed lines respectively), together with the actual moment in our sample (solid line).

Before proceeding with the discussion of individual moments, two comments are worth bearing in mind. First, while these statistics are obtained when all shocks (domestic and foreign) are fed into the model, we have also performed a decomposition by feeding one foreign shock at a time. As mentioned later, this exercise helps us understand which particular disturbances are responsible for the

resulting statistics. Second, and related, when commenting on moments amongst domestic series the results are at times clearer when only all foreign shocks are turned-on. However, to avoid possible confusions in interpreting Figure 7A, we present moments only when all disturbances are active.

Turning to the actual implied moments, the first thing to note is that the prior cross-country correlations in output (top-left panel), inflation (row 2, column 1) and interest rates (row 3, column 1) are positive and in line with the data, albeit lower in the model for interest rates. Therefore, a priori, the model can replicate the substantial comovement observed amongst some variables across Canada and the U.S.

The key point emphasized in section 8 is that generating this comovement implies counterfactual cross-correlations in other series, both across blocks as well as within the domestic block. We organize our discussion of this issue around the shocks mostly responsible for the resulting moments.

Since U.S. preference shocks account for 50 to 70 percent of the variance in U.S. output at different horizons, it is not surprising that these are a priori the main drivers of the cross-country correlation in output alluded to earlier. However, these disturbances also entail a significant negative correlation between Canadian output and both U.S. and Canadian (aggregate) inflation (row 1, columns 2 and 3, respectively), as well as between U.S. output and Canadian inflation (row 1, last column). In the data, these statistics are positive and outside the prior probability bands. Similarly, since U.S. preference shocks explain the largest share of Canadian output variability, these disturbances are also responsible for the counterfactual negative comovement between domestic output and domestic interest rates (row 1, column 4, and, also row 3, column 2). Interestingly, the prior cross-correlation between Canadian output and U.S. interest rates is in line with the data (not shown). Finally, preference shocks induce negative comovement between U.S. output and the terms of trade (row 3, last column) while the correlation in the data is very close to zero.

U.S. cost-push shocks explain three quarters or more of the variance in U.S.

inflation at all horizons. These disturbances a priori capture most of the positive cross-country correlation in inflation rates observed in the data. However, they simultaneously entail positive comovement between U.S. inflation with the real exchange rate (row 3, column 3) and the terms of trade (row 4, column 1). Instead, in the data these moments are somewhat smaller in absolute value, negative and not contained in the prior uncertainty bands.

Similar observations apply to the positive prior link between Canadian inflation and the real exchange rate (row 2, column 3, as well as row 3, column 4) and the terms of trade (row 2, column 4, as well as row 4, column 2). Once again, these statistics in the data are negative. Decomposing these moments across shocks reveals that these two correlations arise partly from U.S. cost-push shocks and partly from U.S. monetary policy disturbances (see below). More generally, when only foreign shocks are fed through the model these two correlations are on average 0.4 or higher.

Regarding U.S. interest rates, U.S. monetary policy shocks account for 80 percent of their variability at shorter horizons, with this share dropping to about 20 percent for the stationary variance (preference shocks, and to a lesser extent technology shocks, explain the remaining long-horizon variability). While their role in international comovement amongst other variables is rather limited, these shocks also induce a positive correlation between domestic inflation with both the terms of trade and the real exchange rate, which as mentioned earlier is counterfactual.

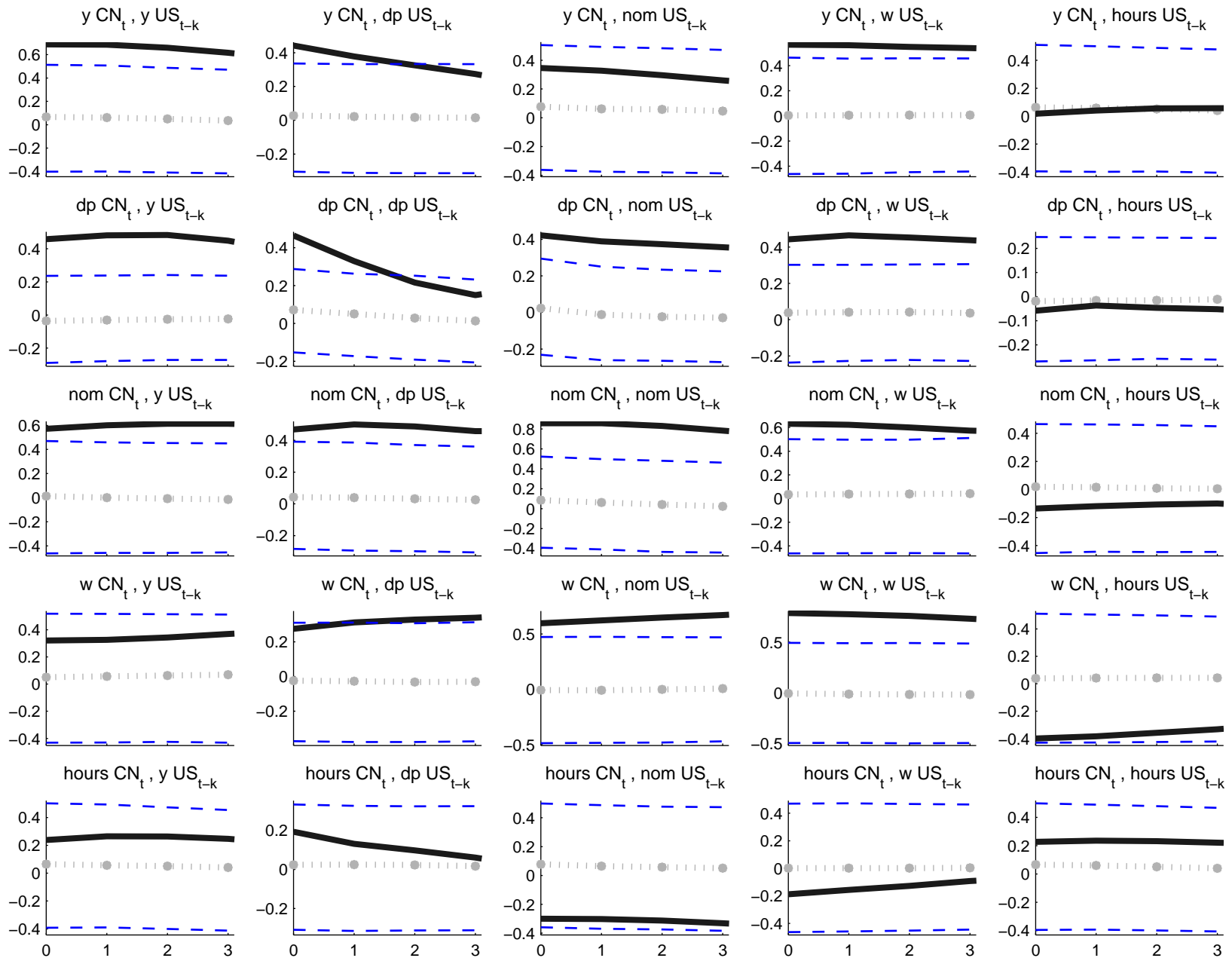
To summarize, we find that while the model can match some prominent cross-country correlations, this comes at the expense of counterfactual predictions in other moments. A number of these problematic a priori implications involve the real exchange rate, terms of trade and inflation. Furthermore, in general the model would seem to entail stronger comovements in the real exchange rate and the terms of trade with a number of Canadian and U.S. series than observed in data, including a counterfactually stronger link with inflation. Overall, this tension between fitting some cross-country correlations at the expense of other

moments helps in part to rationalize why the posterior mode differs so strikingly from the prior with regards to international comovement.

## References

GRANGER, C., H. NAMWON, AND J. YONGIL (2001): “Spurious Regressions with Stationary Series,” *Applied Economics*, 33, 899–904.

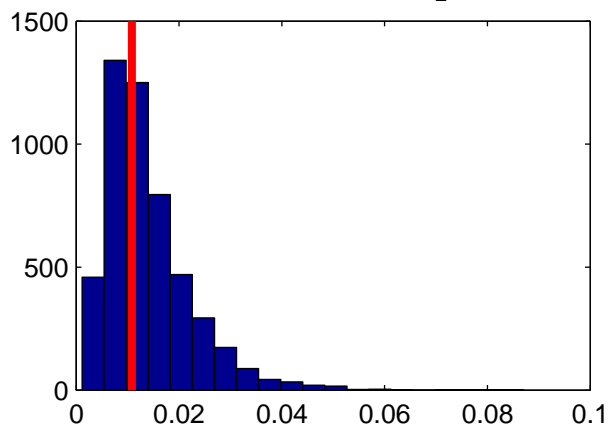
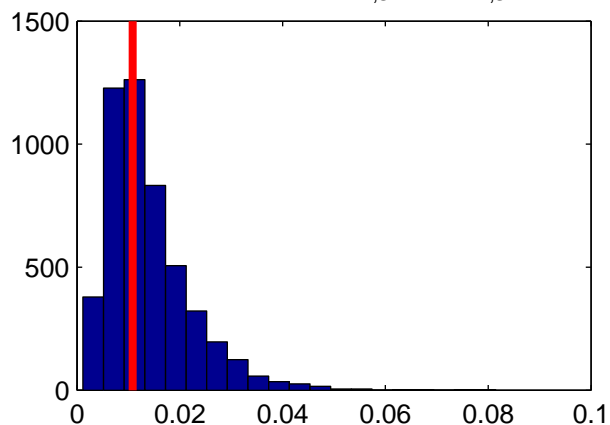
**Figure 1A: Data and simulated DSGE cross-correlations Canada–U.S.**  
**Data (solid), DSGE median (dotted) and [5.95] posterior band (dashed)**



Legend: y (output), dp (inflation), nom (nominal interest rate), w (real wage) and hours.  
 X-axis: k lags of U.S. variables, 0 through 4 (in quarters)

**Figure 2A: Distribution of simulated variance decompositions for CN Output in baseline model**

A. Share foreign shocks with  $V(y_{2,\varepsilon1}) + V(y_{2,\varepsilon2})$  denominator    B. Share foreign shocks with  $V(y_2)$  denominator



C. Share domestic shocks with  $V(y_{2,\varepsilon1}) + V(y_{2,\varepsilon2})$  denominator    D. Variance Ratio  $[V(y_{2,\varepsilon1}) + V(y_{2,\varepsilon2})]/V(y_2)$

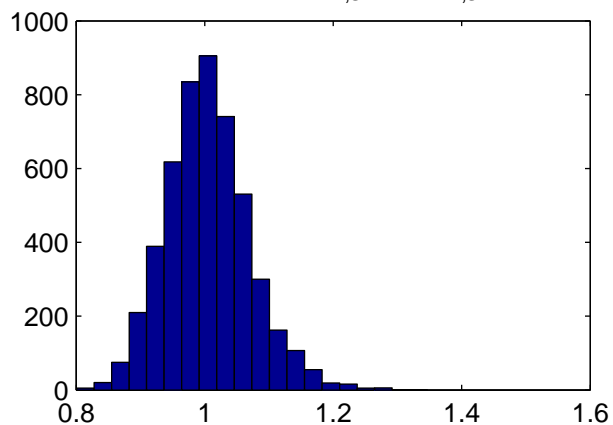
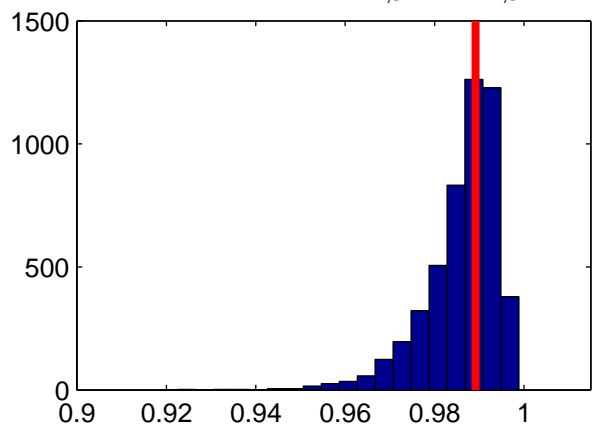
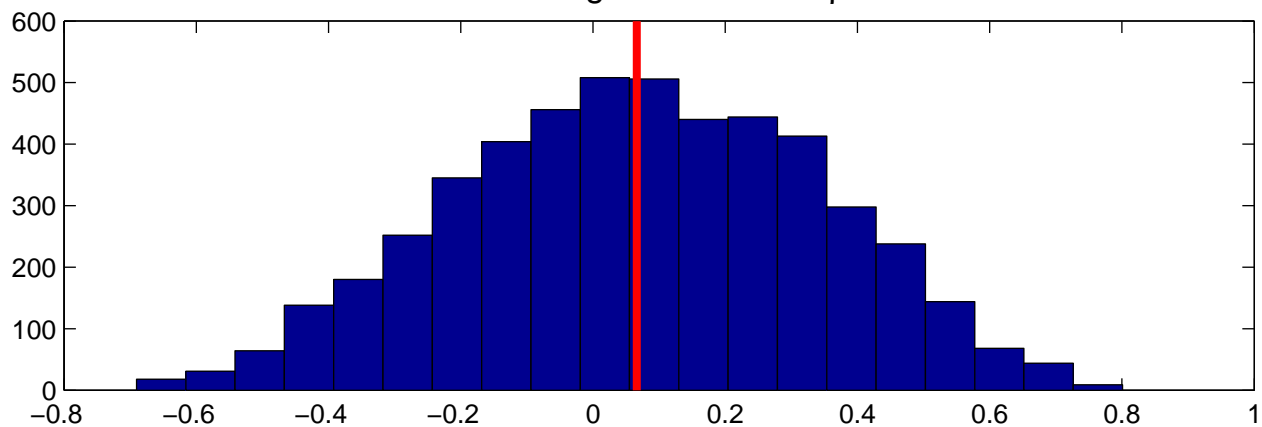


**Figure 3A: Simulated U.S. and C.N. output contemporaneous cross-correlation in baseline model**

A. histogram simulated  $\rho$



B. scatter plot  $|\rho|$  and  $\sqrt{\text{foreign variance share}}$

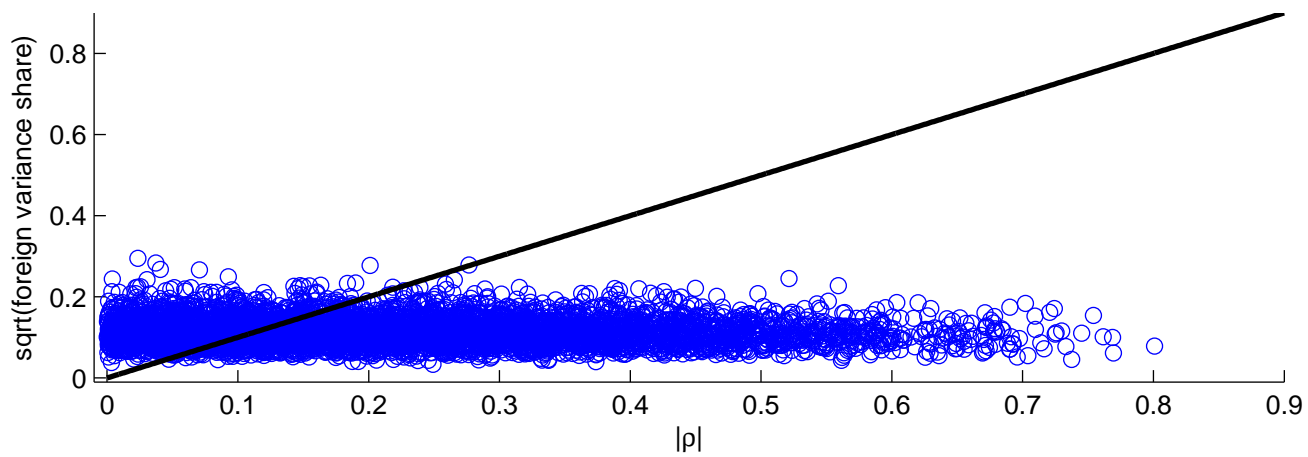


**Figure 4A: Decomposition of contemporaneous output cross-correlation in baseline model**

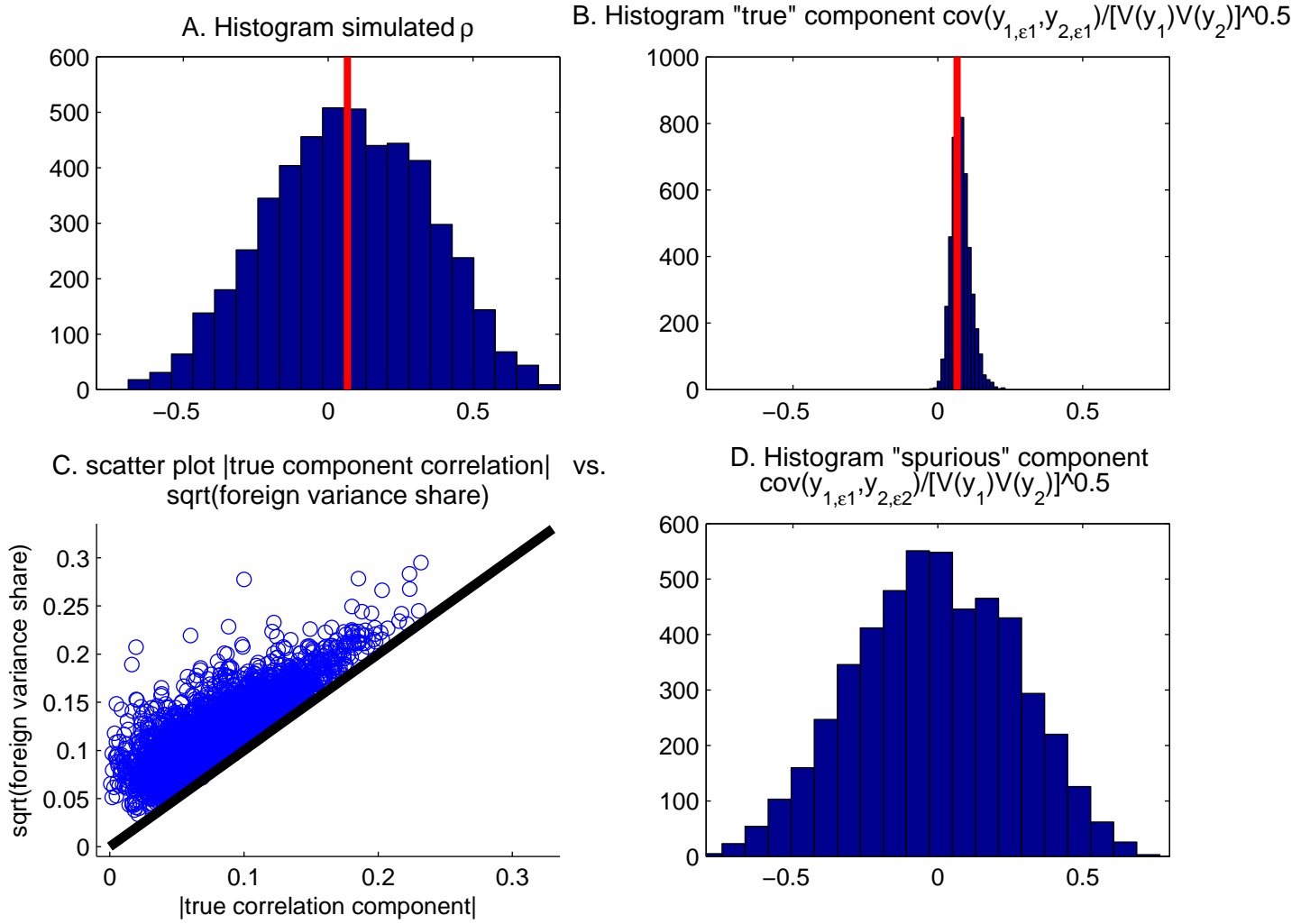
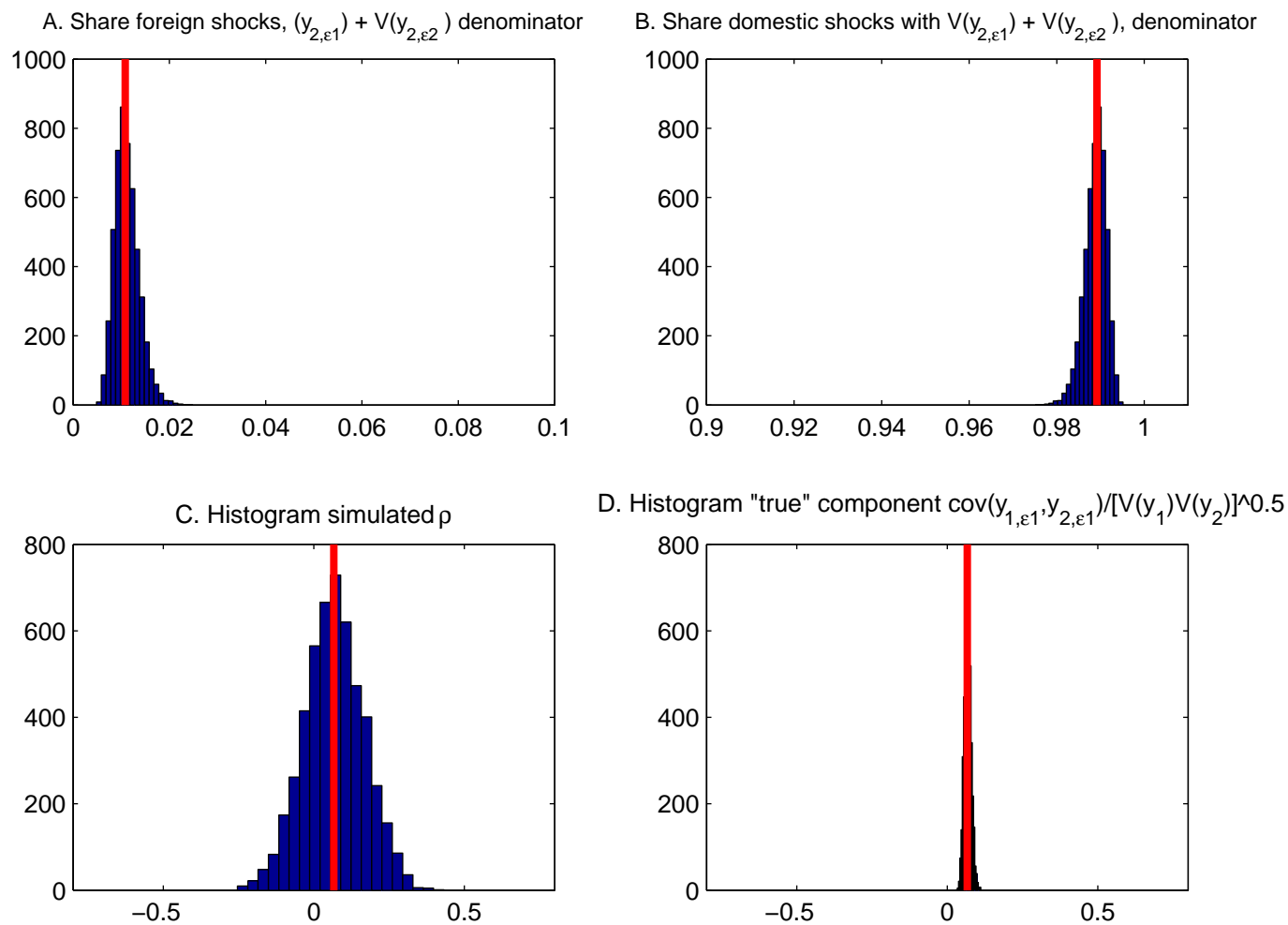
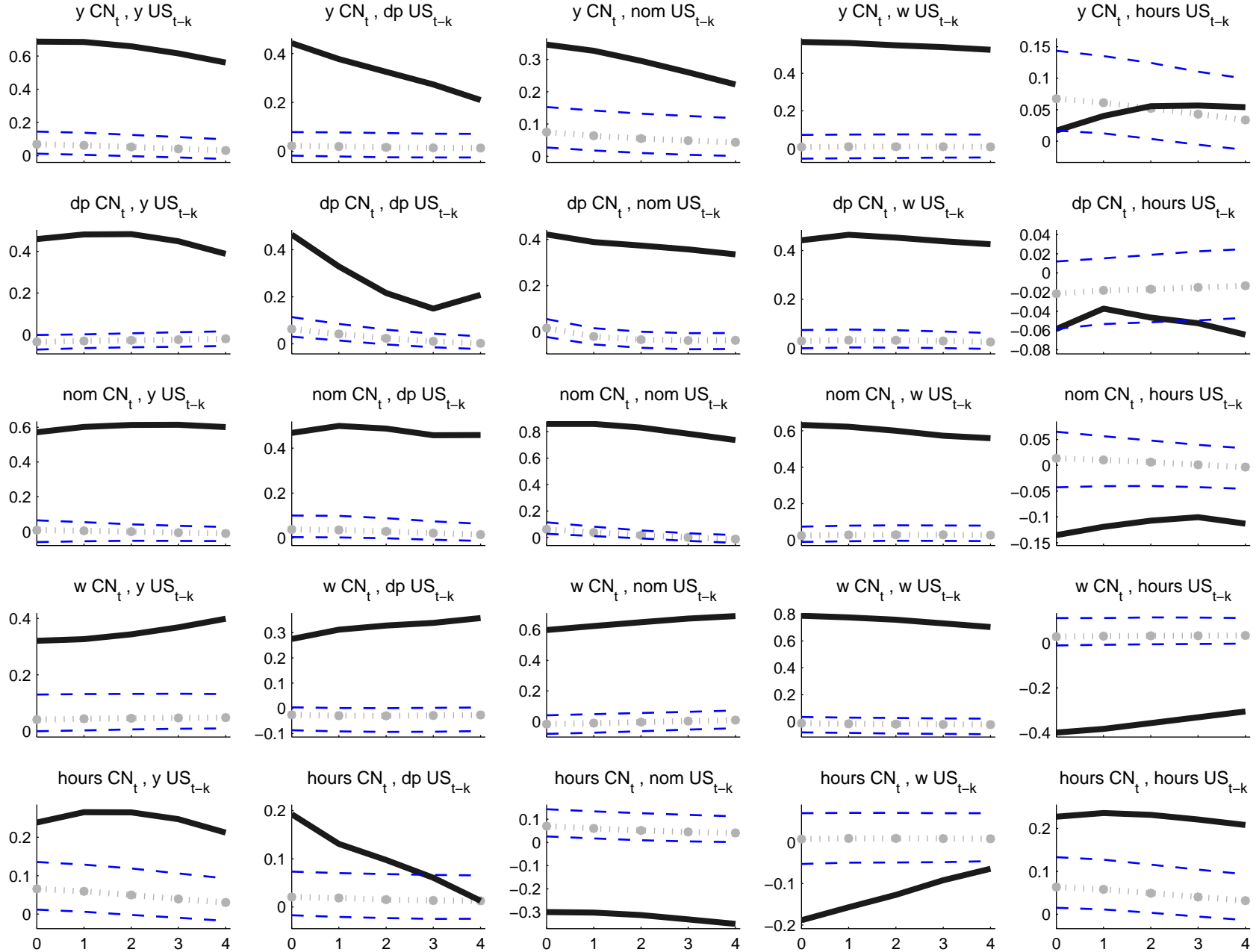


Figure 5A: Simulated CN output variance shares and cross-correlation in baseline model when T=1000



**Figure 6A: Data and simulated DSGE cross-correlations Canada–U.S., "true" components only**  
**Data (solid), DSGE median (dotted) and [5.95] posterior band (dashed)**



Legend: y (output), dp (inflation), nom (nominal interest rate), w (real wage) and hours.  
 X-axis: k lags of U.S. variables, 0 through 4 (in quarters)

**Figure 7A: Selected data & DSGE PRIOR population cross-correlations for model with U.S. block pre-estimated**

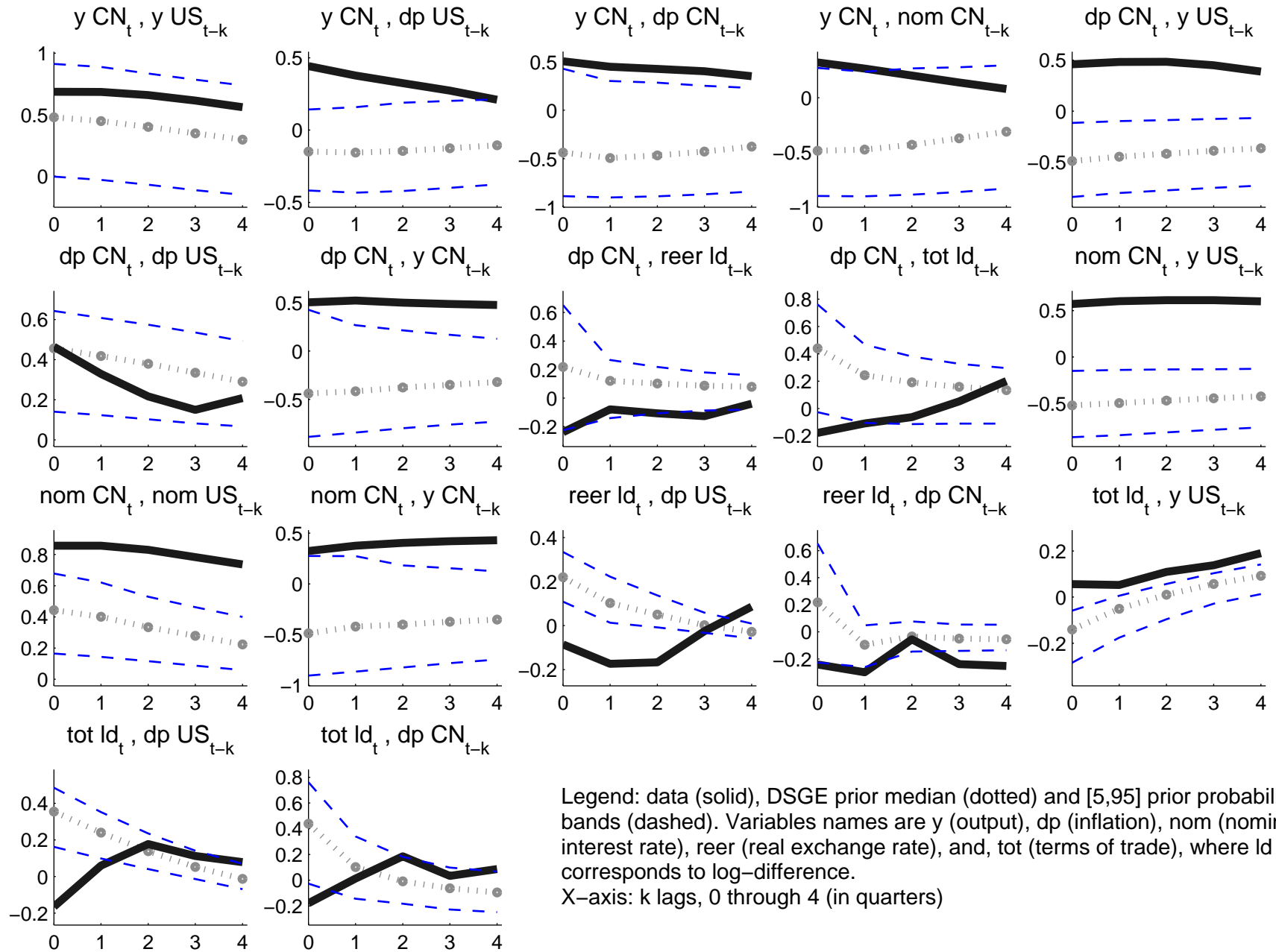


Table 1A: Simulated Posterior Variance Shares<sup>1</sup> of Canadian Series Attributed to All U.S. Shocks in Baseline DSGE

Median and [5,95] posterior bands for all U.S. shocks<sup>2</sup>

Series	Denominator <sup>3</sup>	
	Total Variance	Sum of Foreign and Domestic Variances
Output	0.01 [ 0.00, 0.04]	0.01 [ 0.00, 0.04]
Inflation	0.01 [ 0.01, 0.03]	0.01 [ 0.01, 0.03]
Interest Rate	0.01 [ 0.00, 0.03]	0.01 [ 0.00, 0.03]
Real Wages	0.01 [ 0.00, 0.03]	0.01 [ 0.00, 0.03]
Hours	0.01 [ 0.00, 0.03]	0.01 [ 0.00, 0.03]
Real Exchange Rate	0.03 [ 0.02, 0.05]	0.03 [ 0.02, 0.05]
Terms of Trade	0.05 [ 0.03, 0.09]	0.05 [ 0.03, 0.09]

Notes

<sup>1</sup> Variance shares cover [0,1] interval. Hence 0.01 corresponds to 1 percent.

<sup>2</sup> Computed using the posterior parameter draws reported in table 2 in the paper. In this case, however, the variances are obtained by simulation, rather than using the population formulas from the state space representation of the model's solution as done in table 3. For each posterior parameter draw we generate an artificial sequence of foreign and domestic shocks, of length equal to the sample, in order to simulate the observables.

<sup>3</sup> The variance of each series, which constitutes the denominator of the variance shares, can be obtained in two ways, giving rise to these two columns. First, we refer to the total variance as the simple sample statistic for each observable when all shocks are fed through the model. Second, the denominator can be obtained as the sum of the variance from the series generated when only foreign and only domestic shocks are present. Of course, the second measure will differ from the first due to a small-sample covariance term between components that are orthogonal in population. However, as clearly seen, these considerations do not influence the results.